sensitivity than 121DWHA, 121DWHA/FA, or 121DWHA/PK methods, except for antibody 6H4. Although prolonged exposure of brain material to aldehyde fixatives usually dramatically decreases the antigenicity of PrP^{Sc} [17], this newly enhancing method was more effective for the long-term fixation samples compared with other methods. On the other hand, our simple modification could not enhance immunoreactivity for the prion antigen for antibodies recognizing discontinuous or conformational epitopes.

For immunohistochemical antigen-retrieval techniques, hypotheses such as breaking cross-linking [16], protein denaturation or modification-re-modification [3] have been proposed, and were thought to have an advantage on the basis of observation or support from several studies [18, 22, 23]. In particular, the later theory is based on heat- or chemical-induced modification of the three-dimensional structure of "formalinized" protein, restoring the condition of a formalin-modified protein structure back towards its original structure on the paraffin-embedding tissue sections. Because immunohistochemistry without pretreatment did not give any positive reactions using the pAb B103 and 44B1 in the frozen sections (data not shown), there are some differences between this theory and our model. However, it seemed probable that epitopes hidden by the aggregation of PrPs are exposed on the surface, or that conformational binding sites formed by the other protein molecules are disrupted due to conformational changes induced by the hydrating autoclave methods on the formalin-fixed paraffin sections, assuming that the principle of the antigen-retrieval methods is to lead to a re-naturation or partial restoration of the protein structure with re-establishment of the three-dimensional to something approaching its native condition [22, 23].

Antibody, especially that reacting on the discontinuous epitope, recognizes specific epitopes localized in a spatial configuration within the protein molecule. mAb 15B3 recognizes the discontinuous epitope in the pathological PrP isoform, and a single continuous 15B3 binding site was speculated to be formed either by aggregation of two or several PrP molecules, or by structural rearrangement of a single PrP molecule, or by a combination thereof [12]. The exact mechanisms causing the differences between 135DWHA and 121DWHA methods in the antibody's recognition of the conformational epitope are still unknown. However, these can be surmised as follows: some aggregate proteins or molecules may be loosely arranged and antigenic determinants come to lie on the surface during formic acid or 121°C, 2 atm autoclaving pretreatment; furthermore, elevation of the temperature and atmosphere may cause further changes of certain stereoscopic structures or components of PrP molecules, causing a loss of its conformational epitope. Additional formic acid treatment also causes a slight change, helping in the demasking of the conformational epitope.

Further studies on prion antigen-retrieval techniques, including establishing an exact correlation of these mechanisms and the antibody epitope, may shed new light in the pathology of the prion diseases.

Acknowledgements This work was supported by a Grant-in-Aid for Exploratory Research from the Ministry of Education, Culture, Sports, Science and Technology of Japan (grant 14656118) and a Grant from the Ministry of Health, Labor and Welfare of Japan (grant 14240101).

References

1. Bell JE, Gentleman SM, Ironside JW, McCardle L, Lantos PL, Fergusson J, Luthert P, McQuaid S, Allen IV (1997) Prion protein immunocytochemistry-UK five centre consensus report. Neuropathol Appl Neurobiol 23:26–35
2. Bodemer W (1999) The use of monoclonal antibodies in human prion disease. Naturwissenschaften 86:212–220
3. Cattoretti G, Pileri S, Parravicini C, Becker MHG, Poggi S, Bifulco C, Key G, D'Amato L, Sabattini E, Feudale E, Reynolds F, Gerdes J, Rilke F (1993) Antigen unmasking on formalin-fixed, paraffin-embedded tissue sections. J pathol 171:83–98
4. Doi-Yi R, Kitamoto T, Tateishi J (1991) Immunoreactivity of cerebral amyloidosis is enhanced by protein denaturation treatments. Acta Neuropathol 82:260–265
5. Everbroeck BV, Pals P, Martin JJ, Cras P (1999) Antigen retrieval in prion protein immunohistochemistry. J Histochem Cytochem 47:1465–1467
6. Haritani M, Spencer YI, Wells GAH (1994) Hydrated autoclave pretreatment enhancement of prion protein immunoreactivity in formalin-fixed bovine spongiform encephalopathy-affected brain. Acta Neuropathol 87:86–90
7. Hashimoto K, Mannen T, Nukina N (1992) Immunohistochemical study of kuru plaques using antibodies against synthetic prion protein peptides. Acta Neuropathol 83:613–617
8. Hayward PAR, Bell JE, Ironside JW (1994) Prion protein immunocytochemistry: reliable protocols for the investigation of Creutzfeldt-Jacob disease. Neuropathol Appl Neurobiol 20:375–383
9. Hegyi I, Hainfellner JA, Flicker H, Ironside J, Hauw JJ, Tateishi J, Haltia M, Bugiani O, Aguzzi A, Budka H (1997) Prion protein immunocytochemistry: reliable staining protocol, immunomorphology, and diagnostic pitfalls. Clin Neuropathol 16:262–263
10. Kitamoto T, Ogomori K, Tateishi J, Prusiner SB (1987) Formic acid pretreatment enhances immunostaining of cerebral and systemic amyloids. Lab Invest 57:230–236
11. Kitamoto T, Shin RW, Doh-ura K, Tomokane N, Miyazono M, Muramoto T, Tateishi J (1992) Abnormal isform of prion proteins accumulates in the synaptic structures of the central nervous system in patients with Creutzfeldt-Jakob disease. Am J Pathol 140:1285–1294
12. Korth C, Stierli B, Streit P, Moser M, Schaller O, Fischer R, Schulz-Schaeffer W, Kretzschmar H, Raeber A, Braun U, Ehrensperger F, Hornemann S, Glockshuber R, Rick R, Billeter M, Wüthrich K, Oesch B (1997) Prion (PrP^{Sc})-specific epitope defined by a monoclonal antibody. Nature 390:74–77
13. Kovács GG, Head MW, Hegyi I, Bunn TJ, Flicker H, Hainfellner JA, McCardle L, László L, Jarius C, Ironside JW, Budka H (2002) Immunohistochemistry for the prion protein: comparison of different monoclonal antibodies in human prion disease subtypes. Brain Pathol 12:1–11
14. Liberski PP, Yanagihara R, Brown P, Kordek R, Kloszewska I, Bratosiewicz J, Gajdusek DC (1996) Microwave treatment enhances the immunostaining of amyloid deposits in both the transmissible and non-transmissible brain amyloidoses. Neurodegeneration 5:95–99

15. MacDonald ST, Sutherland K, Ironside JW (1996) A quantitative and qualitative analysis of prion protein immunohistochemical staining in Creutzfeldt-Jacob disease using four anti prion protein antibodies. Neurodegeneration 5:87–94
16. Mason JT, O'Leary TJ (1991) Effects of formaldehyde fixation on protein secondary structure: a calorimetric and infrared spectroscopic investigation. J Histochem Cytochem 39:225–229
17. McBride PA, Bruce ME, Fraser H (1988) Immunostaining of scrapie cerebral amyloid plaques with antisera raised to scrapie-associated fibrils (SAF). Neuropathol Appl Neurobiol 14:325–336
18. Montero C (2003) The antigen-antibody reaction in immunohistochemistry. J Histochem Cytochem 51:1–4
19. Privat N, Sazdovitch V, Seilhean D, Laplanche JL, Hauw JJ (2000) PrP immunohistochemistry: different protocols, including a procedure for long formalin fixation, and a proposed schematic classification for deposits in sporadic Creutzfeldt-Jacob disease. Microsc Res Tech 50:26–31
20. Prusiner SB (1998) Prions. Proc Natl Acad Sci USA 95:13363–13383
21. Ryder SJ, Spencer YI, Bellerby PJ, March SA (2001) Immunohistochemical detection of PrP in the medulla oblongata of sheep: the spectrum of staining in normal and scrapie-affected sheep. Vet Rec 148:7–13
22. Shi S-R, Cote RJ, Taylor CR (1997) Antigen retrieval immunohistochemistry: past, present, and future. J Histochem Cytochem 45:327–343
23. Shi S-R, Cote RJ, Taylor CR (2001) Antigen retrieval techniques: current perspectives. J Histochem Cytochem 49:931–937
24. Wells GAH, Wilesmith JW, McGill IS (1992) Bovine spongiform encephalopathy. Brain Pathol 1:69–78

Available online at www.sciencedirect.com
SCIENCE DIRECT
ELSEVIER
Biochemical and Biophysical Research Communications 335 (2005) 785–792
BBRC
www.elsevier.com/locate/ybbrc

Conformational change in full-length mouse prion: A site-directed spin-labeling study

Osamu Inanami [a,f,g,*], Shukichi Hashida [a,f], Daisuke Iizuka [a], Motohiro Horiuchi [a,f], Wakako Hiraoka [b], Yuhei Shimoyama [c,g,h], Hideo Nakamura [d,g,h], Fuyuhiko Inagaki [e], Mikinori Kuwabara [a]

[a] *Laboratory of Radiation Biology, Department of Environmental Veterinary Medical Sciences, Graduate School of Veterinary Medicine, Hokkaido University, Sapporo 060-0818, Japan*
[b] *Department of Physics, School of Science and Technology, Meiji University, Kawasaki 214-8571, Japan*
[c] *Soft-Matter Physics Laboratory, Department of Materials Science and Engineering, Muroran Institute of Technology, Muroran 050-8585, Japan*
[d] *Laboratory of Chemistry, Faculty of Education, Hokkaido University of Education, Hakodate 040-8567, Japan*
[e] *Department of Structural Biology, Graduate School of Pharmaceutical Sciences, Hokkaido University, Sapporo 060-0812, Japan*
[f] *COE program, Program for Excellence of Zoonosis Control, Sapporo 060-0818, Japan*
[g] *CREST-JST, Multi-Quantum Coherence ESR Project, Muroran 050-8585, Japan*
[h] *CREST-JST, Multi-Quantum Coherence ESR Project, Hakodate 040-8567, Japan*

Received 21 July 2005
Available online 10 August 2005

Abstract

The structure of the mouse prion (moPrP) was studied using site-directed spin-labeling electron spin resonance (SDSL-ESR). Since a previous NMR study by Hornemanna et al., [Hornemanna, Korthb, Oeschb, Rieka, Widera, Wüthricha, Glockshubera, Recombinant full-length murine prion protein, mPrP (23–231): purification and spectroscopic characterization, FEBS Lett. 413 (1997) 277–281] has indicated that N96, D143, and T189 in moPrP are localized in a Cu^{2+} binding region, Helix1 and Helix2, respectively, three recombinant moPrP mutations (N96C, D143C, and T189C) were expressed in an *Escherichia coli* system, and then refolded by dialysis under low pH and purified by reverse-phase HPLC. By using the preparation, we succeeded in preserving a target cystein residue without alteration of the α-helix structure of moPrP and were able to apply SDSL-ESR with a methane thiosulfonate spin label to the full-length prion protein. The rotational correlation times (τ) of 1.1, 3.3, and 4.8 ns were evaluated from the X-band ESR spectra at pH 7.4 and 20 °C for N96R1, D143R1, and T189R1, respectively. τ reflects the fact that the Cu^{2+} binding region is more flexible than Helix1 or Helix2. ESR spectra recorded at various temperatures revealed two phases together with a transition point at around 20 °C in D143R1 and T189R1, but not in N96R1. With the variation of pH from 4.0 to 7.8, ESR spectra of T189R1 at 20 °C showed a gradual increase of τ from 2.9 to 4.8 ns. On the other hand, the pH-dependent conformational changes in N96R1 and D143R1 were negligible. These results indicated that T189 located in Helix2 possessed a structure sensitive to physiological pH changes; simultaneously, N96 in the Cu^{2+} binding region and D143 in Helix1 were conserved.

Keywords: Site-directed spin-labeling; Electron spin resonance; Prion; Conformational change; pH-sensitive region

The cellular prion protein (PrP^c) is a glycosylphosphatidylinositol (GPI)-plasma membrane-anchored protein whose function is still under debate [1–10]. Conversion of PrP^c from an α-helix- to a β-sheet-rich structure (the scrapie prion protein, PrP^{Sc}) causes relevant biophysical changes to the protein that have been related to brain dysfunction in prion diseases [1–3]. The mechanisms involved in the conversion are unknown. However, accumulating evidence suggests that

* Corresponding author. Fax: +81 11 706 7373.
E-mail address: inanami@vetmed.hokudai.ac.jp (O. Inanami).

0006-291X/$ - see front matter © 2005 Elsevier Inc. All rights reserved.
doi:10.1016/j.bbrc.2005.07.148

the process occurs after PrP^c reaches the plasma membrane, and it may involve the entry of PrP^c into intracellular acidic organelles [4–10].

As shown in Fig. 1A, the prion protein of the mouse, moPrP, consists of 208 amino acids (residues 23–231). It contains a carboxy-terminal domain, moPrP (121–231), which represents an autonomous folding unit with three α-helices (Helix1, Helix2, and Helix3) and a two-stranded antiparallel β-sheet [1–3,11–13]. In the full-length prion protein, moPrP (23–231), comparison of near-UV circular dichroism (CD), fluorescence and one-dimensional ^1H NMR spectra of moPrP (23–231) and moPrP (121–231) shows that amino-terminal segment 23–120, which includes the five characteristic octapeptide repeats, does not contribute measurably to the manifestation of the three-dimensional structure as detected [7]. Development of techniques for analysis of the structural and conformational changes in the amino-terminal region of moPrP is of great importance, because the amino-terminal region acts as a Cu^{2+} binding domain [11] and Cu^{2+} ions modulate various biological functions of prions such as the cellular enzymatic activity of superoxide dismutase (SOD) [14], signal transduction [15], shedding of PrP^c [16], and conversion to PrP^{sc} [17]. Recently, site-directed spin labeling (SDSL) together with electron spin resonance (ESR) spectroscopy has proven to be a practical method for determining the secondary structure and molecular orientation; surfaces of tertiary interactions; inter-residue distances and the chain topologies of various proteins [18–21]. SDSL involves the introduction of a spin-labeled side chain into protein sequences, usually through cysteine substitution mutagenesis, followed by reaction with a sulfhydryl-specific nitroxide reagent such as a methane thiosulfonate spin label (MTSSL) (Fig. 1B). Although SDSL-ESR is widely recognized as a useful method for structural analysis and domain dynamics of a number of membrane and soluble proteins, there are no reports about the application of this technique to detection of conformational changes in PrP^c.

In the present study, to obtain information about pH- and temperature-dependent conformational changes of typical domains in PrP, we employed the SDSL-ESR technique. We targeted the amino acid residues

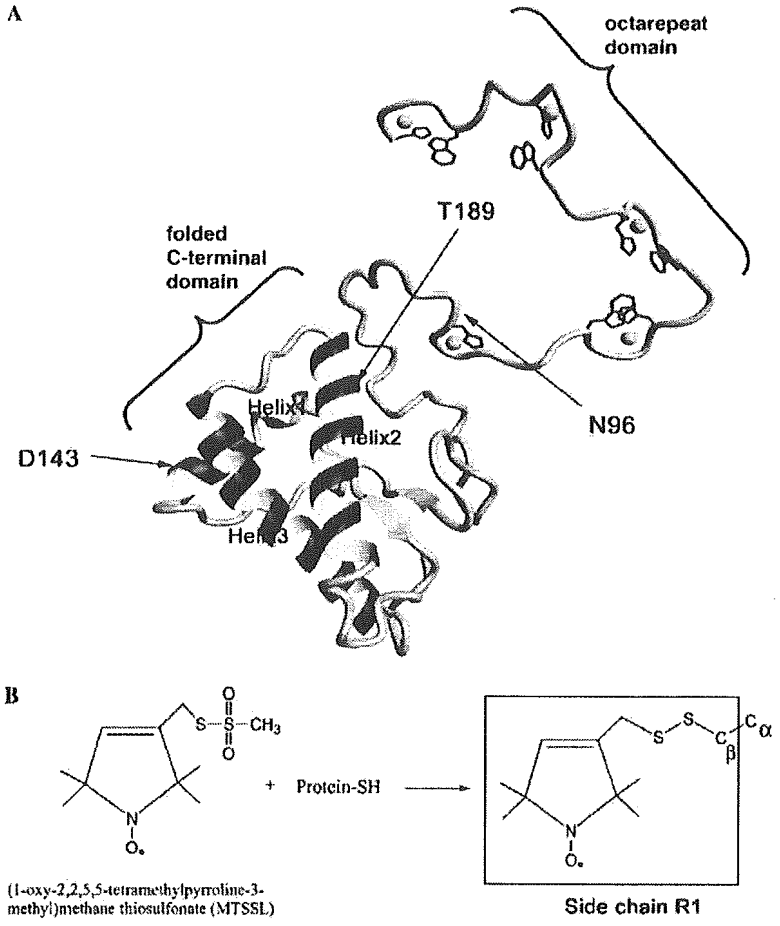

Fig. 1. (A) Three-dimensional rendering of PrP (61–231) [11] and the target sites (N96, D143, and T189) for site-directed spin-labeling (SDSL). (B) The reaction scheme of the methanethiosulfonate spin labeling reagent with cystein residue to yield the R1 side chain attached to the PrP.

of N96, D143, and T189 of recombinant moPrP for the SDSL study, since previous NMR studies have shown that N96, D143, and T189 in moPrP were localized in a Cu^{2+} binding region around H95, Helix1, and Helix2, respectively [7,12,13].

Materials and methods

Materials. (1-Oxy-2,2,5,5-tetramethyl-3-pyrroline-3-methyl)methanethiosulfonate (MTSSL) was purchased from Toronto Research Chemicals (ON, Canada). *Escherichia coli* BL21(DE3)*LysS* and isopropylthio-β-D-galactoside (IPTG) were from Invitrogen (CA, USA). The TSKgel Phenyl-5PW RP column was from TOSOH (Tokyo, Japan). Other reagents were from Wako Pure Chemical (Tokyo, Japan).

Construction of moPrP mutants. cDNA encoding moPrP codons 23–231 was cloned into *Bam*HI/*Eco*RI sites of pRSETb as described previously [22]. To generate the mutant moPrP containing a single amino acid substitution at codon 96 (Asn to Cys), 143 (Asp to Cys) or 189 (Thr to Cys), we used the PCR-based site-directed mutagenesis method described by Imai et al. [23]. The change of the codon by cystein substitution mutagenesis was confirmed using a DNA sequencer (CEQ8800, Beckman).

Expression and purification of recombinant moPrP mutants. The expression plasmids were introduced into *E. coli* BL21(DE3)*LysS*. Protein expression was induced by adding IPTG to a final concentration at 0.5 mM. Four to six hours after induction, bacterial cells were collected and inclusion bodies were prepared as described elsewhere [24]. The inclusion bodies from BL21(DE3)*LysS* transformed with expression plasmids were solubilized with 6 M GdnHCl in 20 mM phosphate buffer (pH 7.8). The recombinant moPrP was further purified by Ni^{2+}-immobilized metal affinity chromatography using Ni^{2+}-charged chelating Sepharose (Qiagen) and a stepwise elution gradient from pH 6.5 to 4.3 in the presence of 8 M urea. After dialysis against 10 mM acetate buffer (pH 4.0) for 48 h, recombinant moPrP containing an intramolecular disulfide bond was purified by reverse-phase HPLC using TSKgel phenyl-5PW RP and a 30–50% linear gradient of acetonitrile with 0.05% trifluoroacetic acid. The purified recombinant moPrP was dialyzed against 10 mM acetate buffer (pH 4.0) and stored at −20 °C until use. The protein concentration was determined by measuring the UV absorption at 276 nm using an extinction coefficient of 39,425 $cm^2\ M^{-1}$. Protein purity was analyzed by sodium dodecyl sulfate–polyacrylamide gel electrophoresis (SDS–PAGE), followed by Commasie brilliant blue staining. All mutants were at least 95% pure as judged by the SDS–PAGE.

Circular dichroism. Far-UV circular dichroism (CD) spectra were recorded on a JASCO J-820 spectropolarimeter with a protein concentration of 0.3 mg/ml in 1 mm pathlength cuvettes using a scan speed of 50 nm/min and a response time of 2 s. Multiple scans were averaged (typically $n = 6$).

Spin-labeling of moPrP mutants. To label the moPrP mutants with MTSSL, a 10-fold molar excess of MTSSL was added to each moPrP mutation in 10 mM acetate buffer (pH 4.5) and the sample was incubated in the dark for 12–24 h at 4 °C for solvent-accessible sites. The free spin label was removed from the protein using a microdialyzer (Nippon Genetics) and spin-labeled moPrP was concentrated by centrifugal concentrator (Vivascience). To confirm the site-specific spin-labeling for the cystein residue created by mutagenesis, the sample solution containing the spin-labeled moPrP mutant was digested for 3–24 h at 37 °C with 1 μg/ml trypsin (Promega) in 50 mM Tris–HCl, pH 8.0, 1 mM $CaCl_2$, and the fragment mass was examined with a matrix-assisted laser desorption ionization (MALDI) mass spectrometer (AutoFLEX, Bruker) equipped with a 337 nm laser source. In all mutants, there was an increase of about $m/z = 184$ by addition of a side chain (R1) of the labeling compound as expected if specifically incorporated MTSSL was detected in each fragment containing the substituted cystein (data not shown).

ESR spectroscopy. The pH change of the sample solution was carried out by dialysis of the sample against 10 mM acetate buffer from pH 4.0 to 6.0 or 10 mM Tris–HCl buffer from pH 6.5 to 8.0. For ESR spectroscopy, 70 μl of spin-labeled moPrP solution was placed into a quartz flat cell (RST-DVT05; 50 mm × 4.7 mm × 0.3 mm, Radical Research). Spectra were detected using a JEOL-RE X-band spectrometer (JEOL) connected with a cylindrical TE011 mode cavity (JEOL). All the ESR spectra were recorded at the temperature range of 5–60 °C maintained by a temperature controller (ES-DVT4, JEOL). We used a field modulation of 0.2 mT operating at 100 kHz, an incident microwave power of 5 mW, and a field sweep of 10 mT. Three field sweeps were averaged for each acquired spectrum by using the Win-Rad Radical Analyzer System (Radical Research). The rotational correlation time (τ) was reported by using the following equation described by Kivelson [25]:

$$\tau(\text{nsec}) = a_0 \delta H_{(0)} \left(\sqrt{h_{(0)}/h_{(+1)}} - 1 \right). \quad (1)$$

Here $\delta H_{(0)}$ is the width of the central peak of the nitroxide signal (in mT); $h_{(0)}$ and $h_{(+1)}$ are the lineheights of the spectral peaks for the quantum numbers of $M = 0$ and $+1$, and we employed a value of 6.5 for the constant a_0. The practical evaluation of τ was performed by the spin-label calculator system of the Win-Rad Radical Analyzer System (Radical Research).

Results

Spin-labeling of recombinant moPrP

For the SDSL-ESR experiment, refolding of recombinant moPrP mutants isolated from inclusion bodies of *E. coli.* was achieved by dialysis against 10 mM acetate buffer (pH 4.0) and the native form of moPrP was isolated by reverse-phase HPLC. The native form of recombinant moPrP is generally defined by the oxidative formation of its single disulfide bond (Cys178–Cys213) and characterized by a typical α-helical far-UV CD spectrum, with minima at 208 and 222 nm [7,26]. These two minima at 208 and 220 nm are reported to disappear if the disulfide bond between Cys179 and Cys214 is destroyed by mutagenesis or treatment with a reducing reagent such as DTT [26]. Therefore, we first recorded far-UV CD spectra of recombinant moPrP mutants in order to confirm that the α-helix content of recombinant moPrP mutants was similar to that of recombinant wild-type moPrP. Fig. 2 shows far-UV CD spectra obtained from wild-type, N96C, D143C, and T189C moPrP. Two minima, at about 208 and 220 nm, typical of mainly a helix structure protein, were clearly observed in all samples and there were no differences in the spectra between wild-type moPrP and moPrP mutants (N96C, D143C, and T189C). Moreover, SDS–PAGE with or without dithiothreitol (DTT) showed that no intermolecular disulfide linkage was produced in any moPrP mutant (data not shown). Therefore, our results indicated that the mutagenesis did not affect the α-helical structure of recombinant PrP by preferential forma-

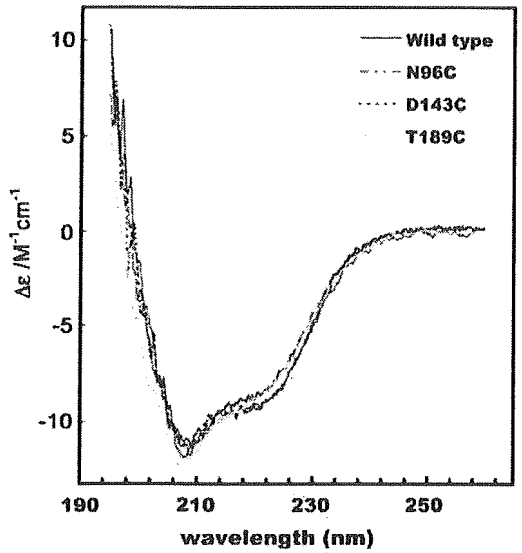

Fig. 2. Circular dichroism (CD) spectra obtained from 0.3 mg/ml moPrP (wild-type), moPrP (N96C), moPrP (D143C), and moPrP (T189C).

tion of a disulfide bond between Cys179 and Cys214, and that the cystein residue created by mutagenesis was preserved during the oxidative refolding.

Temperature-dependent conformational changes of moPrP

The ESR spectra detected from MTSSL bonded with moPrP (wild-type), moPrP (N96C), moPrP (D143C), and moPrP (T189C) are shown in Fig. 3. These ESR spectra are recorded at pH 7.4 at 20 °C. In PrP^{c} (wild-type), no signals derived from the nitroxide radical of MTSSL were detected, indicating that there were no free cystein residues, whereas a triplet ESR signal due to the nitroxide moiety undergoing various dynamic changes was clearly seen in moPrP (N96C), moPrP (D143C), and moPrP (T189C). The rotational correlation times (τ) of 1.1, 3.3, and 4.8 ns were evaluated from these ESR spectra of moPrP (N96C), moPrP (D143C), and moPrP (T189C), respectively. This indicated that the Cu^{2+} binding region was more flexible than the Helix1 region containing D139 or Helix2 containing T189. Furthermore, the line shapes of ESR spectra shown in Figs. 4A–C showed the temperature-dependent variation. There were some peaks in the outermost field of the ESR spectrum of T189R1 at 10 and 20 °C, which were due to the parallel component ($A_{\parallel}$) of the hyperfine tensor. These peaks, as shown by arrows in Fig. 4C, therefore indicated immobilization of the nitroxide moiety in the local region of T189R1. In fact, these peaks vanished at higher temperatures (e.g., 30 °C). The rotational correlation times (τ) were calculated and plotted as a function of temperature at pH 4.4, 6.4, and 7.4 in Figs. 4D–F. In all moPrP mutants, an increase of

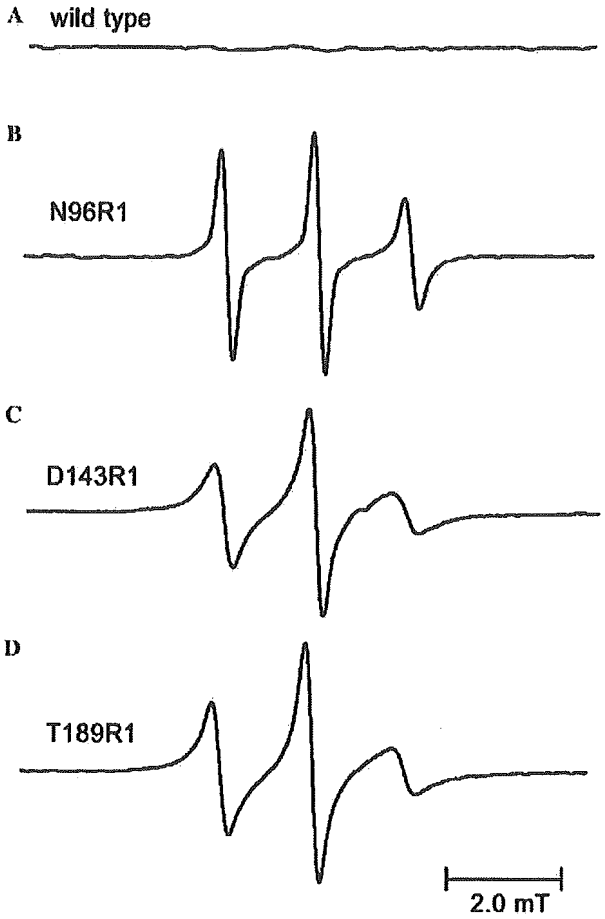

Fig. 3. X-band ESR spectra of spin-labeled recombinant moPrP mutants. After reaction of MTSSL with moPrP (wild-type) (A), moPrP (N96C) (B), moPrP (D143C) (C), and moPrP (T189C) (D), the free spin labeling compound was removed by dialysis against 10 mM acetate buffer (pH 4.0) for 48 h. pH of the sample was adjusted to 7.4 by dialysis against 10 mM Tris–HCl buffer for 4. ESR spectra were recorded by an X-band ESR spectrometer with a field modulation of 0.2 mT, operating at 100 kHz, an incident microwave power of 5 mW and a field sweep of 10 mT.

temperature induced a decrease in τ, which indicated rapid tumbling of the nitroxide moiety. Two phases, a steeper decline of τ at from 5 to 20 °C and a gentle decline at temperatures >20 °C, were observed in moPrP (D143C) and moPrP (T189C) at pH 4.4, 6.4, and 7.4. We found the presence of a breaking point or a phase transition at around 20 °C. The results of slower correlation times found at 10 and 20 °C explain the appearance of $A_{\parallel}$-peaks in the outermost field in moPrP (T189C). However, the phase transition point at 20 °C was not well defined in moPrP (N96C) at any pH.

pH-dependent conformational changes in moPrP

As shown in Fig. 4F, we found a difference in τ between pH 7.4 and 4.4 in moPrP (T189R1), although there were no pH-dependent differences in τ of moPrP

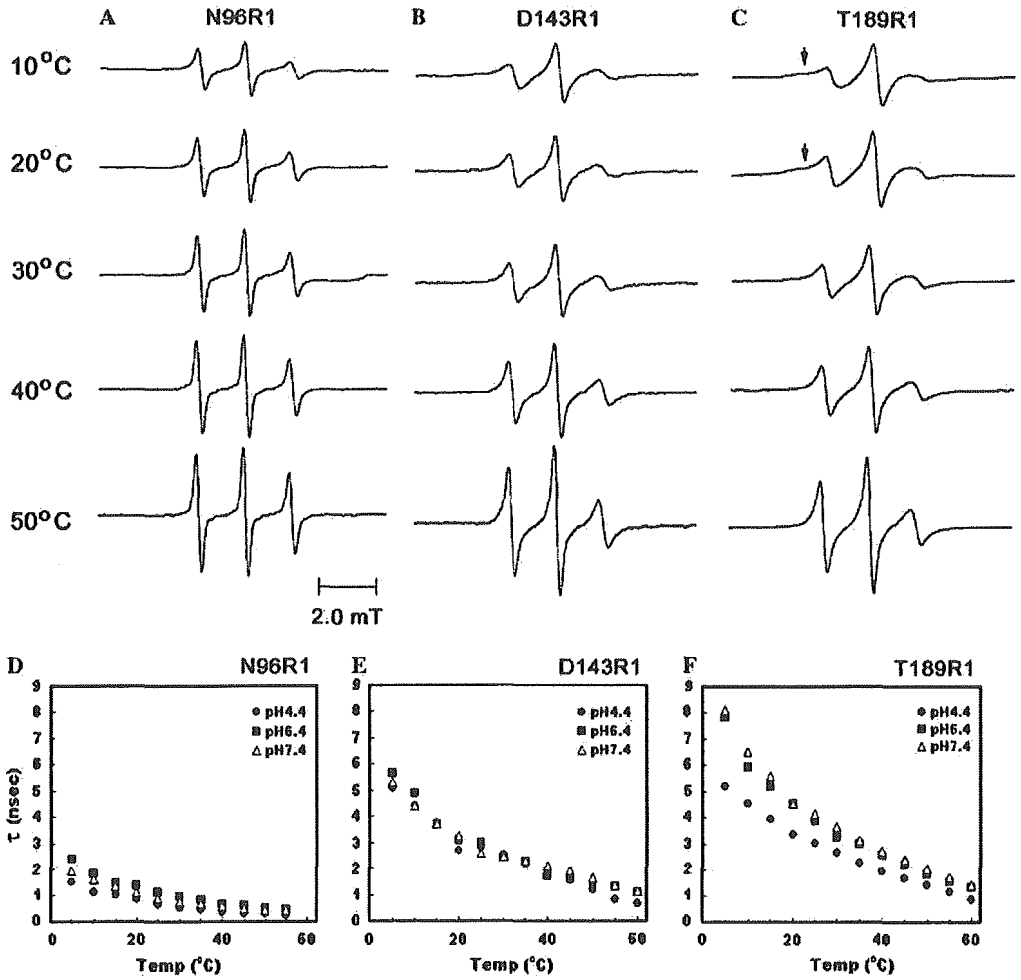

Fig. 4. X-band ESR spectra of recombinant moPrP (N96R1) (A), moPrP (D143R1) (B), and moPrP (T189R1) (C) at 10, 20, 30, 40, and 50 °C. The rotational correlation times, τ (ns), were evaluated from the ESR spectra of moPrP (N96R1) (D), moPrP (D143R1) (E), and moPrP (T189R1) (F) at various temperatures at pH 4.4, 6.4, and 7.4.

(N96C) and moPrP (D143C) as shown in Figs. 4D and E. Fig. 5 shows typical ESR spectra in pH 4.4 solution and pH 7.4 solution of moPrP (T189R1) recorded at 20 °C. The immobilization of the nitroxide moiety at pH 7.4 is obvious in comparison with that at pH 4.4. Furthermore, to define the pH-dependency, we examined the lineshape variation in the ESR spectra of moPrP (T189R1) and moPrP (T189R1) solutions whose pHs were gradually changed from pH 4.0 to 7.8 by dialysis. As shown in Fig. 5B, two regions were observable in moPrP (T189R1), a steep increase phase at pH 4.0–4.8 and a gradual increase phase at pH 5.4–7.8. Stone et al. [27] have also shown similar pH-dependent phase transition at around pH 4.0 in spin-labeled BSA. At temperatures from 5 °C to 20 °C, we found a breaking point between the two phases at around pH 5.0 that was clearer than those seen at temperatures >30 °C. These results indicated that the region around T189R1 was more pH-sensitive than the N96R1 and D189R1 regions.

Discussion

Preparation procedures of SDSL

Site-directed spin labeling is one of the most powerful methods for investigating the structure and conformational switching in soluble and membrane proteins [18,20]. Analysis of nitroxide side chain dynamics in spin-labeled proteins reveals contributions from fluctuations in the backbone, dihedral angles, and rigid-body motions of α-helices [18–21]. With this technique, however it is necessary that free cystein residues be substituted for alanine or serine residues for specificity in the reaction of MTSSL with the target cystein residue created by mutagenesis. The native mouse, hamster, bovine, and human prion proteins do not have free cystein residues, but a disulfide linkage is known to exist between Helix2 and Helix3, and to be essential for formation of three helix structures, which are important in refolding prion secondary structures [26].

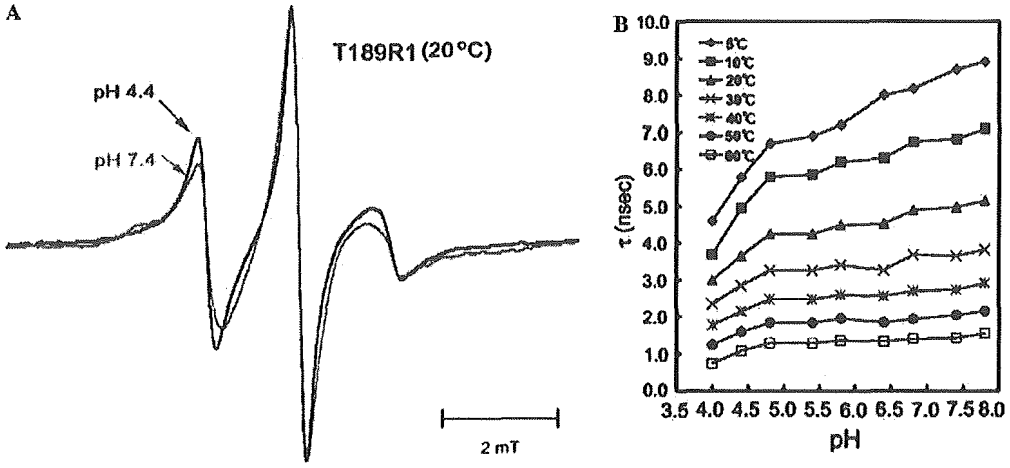

Fig. 5. (A) X-band ESR spectra of moPrP (T189R1) at 20 °C, and pH 4.4 (black line) and pH 7.4 (red line). (B) The rotational correlation time, τ (ns), at various pHs as detected by the ESR spectra of moPrP (T189R1) from 5 to 60 °C. (For interpretation of the references to colour in this figure legend, the reader is referred to the web version of this paper.)

Although Lundberg et al. [28] have reported the time-dependent changes of the ESR spectrum of a short synthetic prion-derived penta-peptide, AGAACAGA with Cys117 substituted for Ala117 in PrP (113–120), there have been few reports on structural analysis by SDSL for the full-length proteins such as PrP having an intracellular disulfide linkage. Application of the SDSL technique is impossible for full-length native PrP protein, because cystein residues newly created by mutagenesis interfere with the formation of the disulfide linkage between Helix2 and Helix3. For this reason, the present experiment employed dialysis against low pH buffer, and reverse-phase HPLC for the refolding and the purification procedures. We demonstrated that the recombinant moPrP produced by this preparation could be successfully used for SDSL experiments as proved by the following evidence. First, far-UV CD spectroscopy, as shown in Fig. 2, clearly demonstrated that the content of the helical structures in moPrP mutants was similar to that in native moPrP. This fact indicates the preferential formation of a disulfide linkage between Cys178 and Cys213, because the abrogation of this disulfide linkage never gives two minima at 208 and 220 nm in far-UV CD spectra [26]. Second, the possibility of dimer formation due to intermolecular disulfide-linkage between cystein residues newly created by mutagenesis was ruled out because SDS–PAGE of recombinant moPrP without the reducing reagent showed a single band (data not shown). Third, MALDI-TOF mass spectroscopic data showed increases of ca. $m/z = 184$ due to a side chain of the nitroxide moiety in the fragment after the tryptic digestion of spin-labeled moPrP mutants (data not shown). Thus, we were able to preserve the target cystein created by mutagenesis and succeeded for the first time in applying SDSL to the full-length prion protein.

Conformational changes of Cu^{2+} binding region and α-helix regions

Prion protein was reported to contain an amino-terminal Cu^{2+} binding octarepeat segment and a carboxy-terminal domain, three α-helices (Helix1, Helix2, and Helix3), and a two-stranded antiparallel β-sheet [1–3,11–13]. The amino acid residues of N96, D143, and T189 in moPrP have been chosen as targets for SDSL. Recently, in addition to the octapeptide repeat region, a novel Cu^{2+} binding structure between H95 and H110 was reported [29] and N96 is close to this region. D143 is located in the initial part of Helix1 and D189 in the end part of Helix2. A marked difference in rotational correlation times was observed by the spin-labeled positions (Fig. 3). NMR data of hamster PrP (90–231) showed that the region from 90 to 124, which includes the characteristic octapeptide repeat sequence, was clearly flexible with large negative NOEs and local correlation times of less than 1 ns. This is due to the fact that residues do not form part of any stable secondary or tertiary fold and are highly flexible [30]. Our ESR spectrum of moPrP (N96R1) also showed that the Cu^{2+} region around H95 reflected more flexible motion as compared with the rigid-body motion of helix structure revealed by ESR-lineshapes from moPrP (D143R1) and moPrP (T189R1).

Our data showed that the end part of Helix2 around T189R1 was highly pH-sensitive compared to the Cu^{2+} binding region around N96R1 and the first part of Helix1 around T189R1 (Figs. 4D–F and 5). The conversion from PrP^{c} to PrP^{Sc} is a post-transcriptional process that appears via the endosome pathway [4,5,9] and/or caveolae-like domains [10], both of which are acidic. Lower pH also accelerates conversion from

PrP^{c} to PrP^{Sc} in a cell-free system [31]. Recently, Swietnicki et al. [32] have shown that incubation of the recombinant prion protein under mildly acidic conditions (pH 5 or below) in the presence of low concentrations of guanidine hydrochloride produces a transition to PrP^{Sc}-like β-sheet-rich oligomers that show fibrillar morphology and increased resistance to proteinase K digestion. Since low pH plays a role in facilitating the conformational change that ultimately results in PrP^{Sc} formation, some parts of Helix2 may be candidates for the pH-sensitive region associated with PrP^{Sc} conversion. In this region, we found a phase transition point at around pH 5.0 as shown in Fig. 5B. This evoked the induction of rapid structural change in the end part of Helix2 below pH 5.0. For analysis of the precise mechanism of pH-induced conformational changes in this region, further studies using the SDSL-ESR technique using a variety of recombinant moPrP mutants created on Helix2 will be necessary.

ESR of spin label dynamics

The mobility of the spin label moiety attached to a protein can be quantified in terms of the rotational correlation times in the case of weakly immobilized labels ($\tau = 10^{-9}$–10^{-10} s). τ is determined by the relative linewidths based upon relaxation theory and is given by Eq. (1) (vide infra). In the equation, the lineheights are used instead of the linewidths, because the former are easy to measure accurately. The constant factor a_0 in Eq. (1) is derived from the g-factor and hyperfine anisotropies. For these reasons, Eq. (1) is only applicable to a spin label signal that possesses three well-defined lines with longitudinal (or up and down) symmetry and no anisotropic outermost lines due to the $g_{\|}$ anisotropy. In the present study, we applied Eq. (1) to the rapid tumbling of the weakly immobilized regime of the spin label dynamics.

Acknowledgments

This work was supported in part by Grants-in-Aid for Basic Scientific Research from the Ministry of Education, Culture, Sports, Science and Technology of Japan [No. 17380178 (O.I.), No. 17580275, and No. 17658126 (M.K.)]. O.I., Y.S., and H.N. thank the Research Grants from COE program and CREST-JST program.

References

[1] S.B. Prusiner, Prions, Proc. Natl. Acad. Sci. USA 95 (1998) 13363–13383.
[2] C. Weissmann, Molecular genetics of transmissible spongiform encephalopathies, J. Biol. Chem. 274 (1999) 3–6.
[3] A. Aguzzi, M. Glatzel, F. Montrasio, M. Prinz, F.L. Heppner, Interventional strategies against prion diseases, Nat. Rev. Neurosci. 2 (2001) 745–749.
[4] B. Caughey, G.J. Raymond, The scrapie-associated form of PrP is made from a cell surface precursor that is both protease- and phospholipase-sensitive, J. Biol. Chem. 266 (1991) 18217–18223.
[5] B. Caughey, G.J. Raymond, D. Ernst, R.E. Race, N-terminal truncation of the scrapie-associated form of PrP by lysosomal protease(s): implications regarding the site of conversion of PrP to the protease-resistant state, J. Virol. 65 (1991) 6597–6603.
[6] A. Taraboulos, M. Scott, A. Semenov, D. Avrahami, L. Laszlo, S.B. Prusiner, D. Avrahami, Cholesterol depletion and modification of COOH-terminal targeting sequence of the prion protein inhibit formation of the scrapie isoform, J. Cell Biol. 129 (1995) 121–132.
[7] S. Hornemanna, C. Korthb, B. Oeschb, R. Rieka, G. Widera, K. Wüthricha, R. Glockshubera, Recombinant full-length murine prion protein, mPrP (23–231): purification and spectroscopic characterization, FEBS Lett. 413 (1997) 277–281.
[8] A.C. Magalhaes, J.A. Silva, K.S. Lee, V.R. Martins, V.F. Prado, S.S. Ferguson, M.V. Gomez, R.R. Brentani, M.A. Prado, Endocytic intermediates involved with the intracellular trafficking of a fluorescent cellular prion protein, J. Biol. Chem. 277 (2002) 33311–33318.
[9] D.R. Borchelt, A. Taraboulos, S.B. Prusiner, Evidence for synthesis of scrapie prion proteins in the endocytic pathway, J. Biol. Chem. 267 (1992) 16188–16199.
[10] M. Vey, S. Pilkuhn, H. Wille, R. Nixon, S.J. DeArmond, E.J. Smart, R.G. Anderson, A. Taraboulos, S.B. Prusiner, Subcellular colocalization of the cellular and scrapie prion proteins in caveolae-like membranous domains, Proc. Natl. Acad. Sci. USA 93 (1996) 14945–14949.
[11] C.S. Burns, E. Aronoff-Spencer, G. Legname, S.B. Prusiner, W.E. Antholine, G.J. Gerfen, J. Peisach, G.L. Millhauser, Copper coordination in the full-length, recombinant prion protein, Biochemistry 42 (2003) 6794–6803.
[12] M. Billeter, R. Riek, G. Wider, S. Hornemann, R. Glockshuber, K. Wuthrich, Prion protein NMR structure and species barrier for prion diseases, Proc. Natl. Acad. Sci. USA 94 (1997) 7281–7285.
[13] R. Riek, S. Hornemann, G. Wider, M. Billeter, R. Glockshuber, K. Wuthrich, NMR structure of the mouse prion protein domain PrP (121–321), Nature 382 (1996) 180–182.
[14] W. Rachidi, D. Vilette, P. Guiraud, M. Arlotto, J. Riondel, H. Laude, S. Lehmann, A. Favier, Expression of prion protein increases cellular copper binding and antioxidant enzyme activities but not copper delivery, J. Biol. Chem. 278 (2003) 9064–9072.
[15] C. Spielhaupter, H.M. Schatzl, PrP^{C} directly interacts with proteins involved in signaling pathways, J. Biol. Chem. 276 (2001) 44604–44612.
[16] E.T. Parkin, N.T. Watt, A.J. Turner, N.M. Hooper, Dual mechanisms for shedding of the cellular prion protein, J. Biol. Chem. 279 (2004) 11170–11178.
[17] N. Hijazi, Y. Shaked, H. Rosenmann, T. Ben-Hur, R. Gabizon, Copper binding to PrP^{C} may inhibit prion disease propagation, Brain Res. 993 (2003) 192–200.
[18] W.L. Hubbell, C. Altenbach, C.M. Hubbell, H.G. Khorana, Rhodopsin structure, dynamics, and activation: a perspective from crystallography, site-directed spin labeling, sulfhydryl reactivity, and disulfide cross-linking, Adv. Protein Chem. 63 (2003) 243–290.
[19] R. Biswas, H. Kuhne, G.W. Brudvig, V. Gopalan, Use of EPR spectroscopy to study macromolecular structure and function, Sci. Prog. 84 (2001) 45–67.
[20] W.L. Hubbell, D.S. Cafiso, C. Altenbach, Identifying conformational changes with site-directed spin labeling, Nat. Struct. Biol. 7 (2000) 735–739.

[21] H.S. Mchaourab, M.A. Lietzow, K. Hideg, W.L. Hubbell, Motion of spin-labeled side chains in T4 lysozyme. Correlation with protein structure and dynamics, Biochemistry 35 (1996) 7692–76704.
[22] C.L. Kim, A. Umetani, T. Matsui, N. Ishiguro, M. Shinagawa, M. Horiuchi, Antigenic characterization of an abnormal isoform of prion protein using a new diverse panel of monoclonal antibodies, Virology 320 (2004) 40–51.
[23] Y. Imai, Y. Mastushima, T. Sugimura, M. Terada, A simple and rapid method for generating a deletion by PCR, Nucleic Acid Res. 19 (1991) 2785.
[24] J. Sambrook, E.F. Fritsch, T. Maniatis, Molecular Cloning: A Laboratory Manual, Cold Spring Harbor Press, Cold Spring Harbor, NY, 1989.
[25] D. Kivelson, Theory of ESR linewidths of free radicals, J. Chem. Phys. 33 (1960) 1094–1106.
[26] N.R. Maiti, W.K. Surewicz, The role of disulfide bridge in the folding and stability of the recombinant human prion protein, J. Biol. Chem. 276 (2001) 2427–2431.
[27] T.J. Stone, T. Buckman, P.L. Nordio, H.M. McConnel, Spin-labeled biomolecules, Proc. Natl. Acad. Sci. USA 54 (1965) 1010–1017.
[28] K.M. Lundberg, C.J. Stenland, F.E. Cohen, S.B. Prusiner, G.L. Millhauser, Kinetics and mechanism of amyloid formation by the prion protein H1 peptide as determined by time-dependent ESR, Chem. Biol. 4 (1997) 345–355.
[29] C.E. Jones, S.R. Abdelraheim, D.R. Brown, J.H. Viles, Preferential Cu^{2+} coordination by His96 and His111 induces beta-sheet formation in the unstructured amyloidogenic region of the prion protein, J. Biol. Chem. 279 (2004) 32018–32027.
[30] H. Liu, S. Farr-Jones, N.B. Ulyanov, M. Llinas, S. Marqusee, D. Groth, F.E. Cohen, S.B. Prusiner, T.L. James, Solution structure of Syrian hamster prion protein rPrP (90–231), Biochemistry 38 (1999) 5362–5377.
[31] D.A. Kocisko, S.A. Priola, G.J. Raymond, B. Chesebro, P.T.Jr. Lansbury, B. Caughey, Species specificity in the cell-free conversion of prion protein to protease-resistant forms: a model for the scrapie species barrier, Proc. Natl. Acad. Sci. USA 92 (1995) 3923–3927.
[32] W. Swietnicki, M. Morillas, S.G. Chen, P. Gambetti, W.K. Surewicz, Aggregation and fibrillization of the recombinant human prion protein huPrP90–231, Biochemistry 39 (2000) 424–431.

Suppression of Proliferation of Poliovirus and Porcine Parvovirus by Novel Phenoxazines, 2-Amino-4,4α-dihydro-4α-7-dimethyl-3*H*-phenoxazine-3-one and 3-Amino-1,4α-dihydro-4α-8-dimethyl-2*H*-phenoxazine-2-one

Akiko IWATA,[a] Teruhide YAMAGUCHI,[a] Kouei SATO,[b] Noriko YOSHITAKE,[c] and Akio TOMODA*[,d]

[a] *Division of Cellular and Gene Therapy Products, National Institute of Health, Sciences; 1–18–1 Kamiyoga, Setagaya-ku, Tokyo 158–0098, Japan;* [b] *The Institute of Saitama Red Cross Cente; 8–3–41 Kamiochiai, Saitama, Saitama 338–0001, Japan;* [c] *Third Department of Internal Medicine, Tokyo Medical University; and* [d] *Department of Biochemistry and Intractable Immune System Disease Research Center, Tokyo Medical University; 6–1–1 Shinjuku, Tokyo 160–0022, Japan.*
Received October 7, 2004; accepted January 5, 2005

The present study aimed at investigating the antiviral effects of 2-amino-4,4α-dihydro-4α-7-dimethyl-3*H*-phenoxazine-3-one (Phx-1) and 3-amino-1,4α-dihydro-4α-8-dimethyl-2*H*-phenoxazine-2-one (Phx-2) on 6 representative viruses: poliovirus, porcine parvovirus, simian virus 40 (SV-40), herpes simplex virus-1 (HSV-1), Sindbis virus, and vesicular stomatitis virus (VSV). Phx-1 and Phx-2 suppressed the proliferation of poliovirus in Vero cells and that of porcine parvovirus in ESK cells at concentrations between 0.25 μg/ml and 2 μg/ml, when the cells were treated with Phx-1 and Phx-2 for 1 h and then inoculated with these viruses. The proliferation of the other viruses, SV-40, HSV-1, Sindbis virus, and VSV, in the host cells was not influenced by Phx-1 or Phx-2 at concentrations less than 20 μg/ml. The results suggest that Phx-1 and Phx-2 may be useful to prevent the proliferation of poliovirus and porcine parvovirus infection and may contribute to developing new antiviral drugs in future.

Key words phenoxazine; poliovirus; porcine parvovirus

The development of antiviral drugs has been undertaken in parallel with that of vaccines, so as to overcome viral infections. Vaccination has been adopted to prevent several viral infections due to poliovirus, poxvirus, influenza virus *etc.* However, the usefulness of the antiviral drugs discovered so far seems to be restricted by the adverse effects of the drugs and the appearance of drug-resistant viruses.[1,2]

On the other hand, Tomoda *et al.* found that relatively water-soluble phenoxazines were biosynthesized by the reaction of *o*-aminophenol and its derivatives with human and bovine hemoglobin.[3—5] Among these phenoxazines, 2-amino-4,4α-dihydro-4α-7-dimethyl-3*H*-phenoxazine-3-one (Phx-1) has been demonstrated to have anticancer activity.[6,7] It was also shown that Phx-1 exerts an immunosuppressive effect on the activated lymphocytes such as B cells and T cells[8,9] and the activated mast cells.[10] Therefore, it seems of interest to investigate the effects of water-soluble phenoxazines on the proliferation of viruses in the host cells. We briefly reported that the proliferation of poliovirus inoculated to Vero cells was inhibited by Phx-1.[11] This discovery prompted us to investigate the effects of water-soluble phenoxazines on various kinds of viruses, because there is a possibility that a new antiviral drug may be developed through such an investigation. The present manuscript deals with studies on the antiviral effects of Phx-1 and 2-amino-4,4α-dihydro-4α-7-dimethyl-3*H*-phenoxazine-3-one (Phx-2) on 6 representative viruses: poliovirus, porcine parvovirus, simian virus (SV-40), herpes simplex virus-1 (HSV-1), Sindbis virus, and vesicular stomatitis virus (VSV).

MATERIALS AND METHODS

Phx-1, Phx-2, Cells and Viruses Phx-1 and Phx-2 were prepared by reaction of bovine hemoglobin with 2-amino-5-methylphenol and 2-amino-4-methylphenol, respectively, as previously described.[4,5] The chemical structures of Phx-1 and Phx-2 are shown in Fig. 1. Phx-1 or Phx-2 was dissolved in dimethyl sulfoxide (DMSO) before use to reach a concentration of 20 mM, and then was diluted with α-minimum essential medium (α-MEM).

African green monkey kidney cells (Vero cells), were generously supplied by the Japanese Cancer Research Resources Bank (Tokyo, Japan). The ESK cells (embryonic swine kidney cells line)[12] were kindly donated by Dr. J. Koga (JCR Co., Japan).

Cells were maintained in α-MEM supplemented with 10% fetal calf serum (FCS, Sigma Co., Ltd., St. Louis, MO, U.S.A.), and 30 mg/l kanamycin sulfate RPMI 1640 medium containing 10% heat-inactivated FCS, at 37 °C under moisturized air containing 5% CO_2.

Poliovirus (strain Sabin 1) was also donated by Dr. Koga. Porcine parvovirus (strain 90HS), SV-40, Sindbis virus, and HSV-1 (strain F) were the generous donation of Dr. M. Kohase (National Institute of Infectious Diseases). VSV (strain NJ) was the gift of Dr. H. Kita (Suntory Center Institute, Japan).

The supernatants of Vero cells infected with poliovirus, HSV-1, Sindbis virus, and VSV were used as the virus samples. The supernatant of ESK cells infected with porcine parvovirus was used as the porcine parvovirus sample. CV-1 cells were infected with SV-40 virus, and then 5 d after infec-

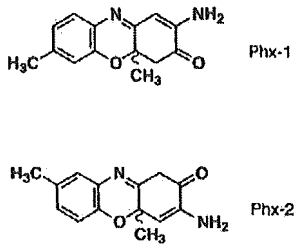

Fig. 1. Chemical Structures of Phx-1 and Phx-2

* To whom correspondence should be addressed. e-mail: tomoda@tokyo-med.ac.jp

Table 1. Effects of Phx-1 or Phx-2 on the Proliferation of Poliovirus Inoculated to Vero Cells at Different Concentrations of Phx-1 and Phx-2, Estimated by $TCID_{50}$[a]

	Phx-1 (μg/ml)					Phx-2 (μg/ml)				
	0	0.25	0.55	1	2	0	0.25	0.5	1	2
$TCID_{50}$	62	32	32	16	17	63	63	63	63	14

a) $TCID_{50}$ was defined as dilution ratio of the virus to generate 50% disruption of the cells.

tion, the supernatant was saved as the SV-40 sample. To remove the cell debris from the collected virus suspension, each suspension was centrifuged at 450×*g* for 10 min. After removing the debris, the resulting stock viruses were aliquoted and stored at −80 °C until use.

Determination of Viral Infectivity The infectious titer of virus suspension was determined using indicator cells. Poliovirus and porcine parvovirus were introduced into Vero cells and ESK cells, respectively.[13] The cells were seeded in a 96-well microplate (Asahi Technoglass Co., Ltd., Tokyo) at a density of 2×10^5 to 3×10^5 cells per well in culture medium. They were then cultured at 37 °C, for 2 d. Various concentrations of Phx-1 or Phx-2 solution [final concentration: 0 μg/ml (DMSO alone), 0.25, 0.5, 1 and 2 μg/ml] were then added to the cells in each well, and these were subsequently incubated for 1 h. After 1 h, the supernatant was removed from the well by an aspirator. At this time, poliovirus or porcine parvovirus which had been serially diluted with α-MEM to obtain a 50% tissue culture infectious dose ($TCID_{50}$, defined as dilution ratio of the virus to generate 50% disruption of the cells), as performed conventionally,[2] was added to Vero cells or ESK cells, respectively, in each well. Cell cultures were incubated for 1 h at 37 °C. Post infection $TCID_{50}$ cultures were then fed with α-MEM containing various concentrations of Phx-1 or Phx-2 [final concentration: 0 (DMSO alone), 0.25, 0.5, 1 and 2 μg/ml] and were incubated at 37 °C for 2 or 3 d.

After that period, the disruption of Vero cells or ESK cells was examined by the method described by Satoh *et al.*,[14] and the infectivity of poliovirus or porcine parvovirus to these cells was estimated. The estimation of the viruses SV-40, HSV-1, Sindbis virus and VSV was essentially in agreement with the method described by Satoh *et al.*[14]

Effects of Phx-1 and Phx-2 on Cell Viability We examined the effects of Phx-1 and Phx-2 on the viability of Vero cells, ESK cells, and CV-1 cells in the presence of various concentrations of these phenoxazines and without addition of viruses. There was no significant disruption of these cells at various concentrations of Phx-1 and Phx-2 up to 50 μg/ml, indicating that these phenoxazines do not affect the viability of the cells at the concentrations of used to examine the viruses.

RESULTS AND DISCUSSION

We initially studied the effects of Phx-1 and Phx-2 on the proliferation of poliovirus, a non-enveloped and single strand RNA virus, inoculated to Vero cells. Since $TCID_{50}$ is defined as the dilution ratio of the virus to generate 50% disruption of the cells, a lower value of $TCID_{50}$ means that the viral proliferation is being suppressed in the host cells. We found that

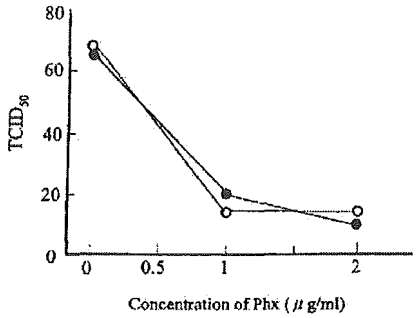

Fig. 2. Antiviral Effects of Phx-1 and Phx-2 on Porcine Parvovirus

The infectious titer of porcine parvovirus suspension was determined using ESK cells, as described in Materials and Methods. Antiviral effects of Phx-1 (●) or Phx-2 (○) were expressed by $TCID_{50}$ (defined as dilution ratio of the virus to generate 50% disruption of the cells) at different concentrations of these phenoxazines (μg/ml of Phx-1 or Phx-2).

$TCID_{50}$ of poliovirus was decreased according to the increase in the concentrations of Phx-1 or Phx-2 (Table 1). Namely, Phx-1 suppressed the proliferation of poliovirus inoculated to Vero cells at all concentrations tested between 0.25 μg/mg and 2 μg/ml, and reached maximal antiviral activity at 1 μg/ml. Phx-2 also inhibited the proliferation of poliovirus inoculated to Vero cells at 2 μg/ml (Table 1). Such inhibition was observed when the cells were treated with Phx-1 or Phx-2 for 1 h and then inoculated with poliovirus. On the contrary, the proliferation of poliovirus was not suppressed by Phx-1 or Phx-2 when Vero cells were inoculated with the virus together with various concentrations of Phx-1 or Phx-2 (data not shown). These results may be explained by the facts that these phenoxazines do not exert virucidal activity against poliovirus directly, but some mechanisms preventing the attachment or the intracellular proliferation of poliovirus in the host cells, are apparently revoked during 1 h incubation of the host cells with Phx-1 or Phx-2. The detailed biochemical changes in the host cells are not yet clear.

Figure 2 shows the inhibitory effects of Phx-1 and Phx-2 against porcine parvovirus, a non-enveloped and single strand DNA virus, as determined by the changes in $TCID_{50}$. These phenoxazines showed antiviral effects on porcine parvovirus at 1 μg/ml and 2 μg/ml. Such inhibition was observed when the cells were treated with Phx-1 or Phx-2 for 1 h and then inoculated with porcine parvovirus. However, Phx-1 or Phx-2 did not exert antiviral effects on porcine parvovirus when ESK cells were inoculated with the virus together with Phx-1 or Phx-2 (data not shown).

We studied the effects of Phx-1 and Phx-2 on various representative viruses such as SV-40 (non-enveloped, double strand DNA), HSV-1 (enveloped, double strand DNA), Sindbis virus (enveloped, single and plus strand RNA), and VSV (enveloped, single strand RNA). Table 2 summarizes the

Table 2. Antiviral Activity of Phx-1 and Phx-2 on Various Species of Viruses

Type of virus	Name of virus	Antiviral activity[a]	
		Phx-1	Phx-2
sDNA, envelope (−)	Porcine parvovirus	+	+
dDNA, envelope (−)	Simian virus 40	−	−
dDNA, envelope (+)	Herpes simplex virus-1	−	−
sRNA, envelope (−) (plus strand)	Poliovirus	+	+
sRNA, envelope (+) (plus strand)	Sindbis virus	−	−
sRNA, envelope (+) (minus strand)	Vesicular stomatitis virus	−	−

a) $TCID_{50}$ was estimated as described in Materials and Methods. Then, the antiviral activity was expressed by + or −, where + shows "effective" at the concentration of Phx-1 or Phx-2 between 0.25 and 20 μg/ml, and − shows "not effective" at these concentrations.

inhibitory effects of Phx-1 and Phx-2 on these viruses, in comparison with poliovirus and porcine parvovirus. Although Phx-1 and Phx-2 showed antiviral activity against poliovirus and porcine parvovirus, these phenoxazines did not inhibit the proliferation of SV-40, HSV-1, Sindbis virus or VSV in the host cells. Therefore, it may be conceivable that non-enveloped and single strand RNA virus (coxackie virus, ECHO virus, hepatitis virus A, encephalomyocarditis virus *etc.*) or non-enveloped and single strand DNA virus (B19 virus, adeno-associated virus 2 *etc.*) may be inhibited by Phx-1 and Phx-2 as well. Increased amounts of interferon is not possible, because the inhibition of proliferation of viruses was restricted only to poliovirus and porcine parvovirus (Table 2). These views should be assessed by further examinations.

Tang *et al.*[15] reported that hypericin, a derivative of emodin exerts antiviral activity against enveloped viruses such as HSV-1, influenza virus A and Mo-Mul V, but not against the non-enveloped viruses poliovirus and adenovirus, at concentrations of 1.56 to 25 μg/ml. On the other hand, our results showed that Phx-1 and Phx-2 exerted antiviral activity only against poliovirus and porcine parvovirus (Table 1, Fig. 2). Concerning the chemical structure of emodin (1,3,8-trihydroxy-6-methylanthraquinone) and Phx-1, emodin is analogous to Phx-1, because emodin and Phx-1 (Fig. 1) are tricyclic chromophores with the methyl group at the same position, however, the former is a semiquinone type producing active oxygens,[16] while the latter is a non-semiquinone type. Such similarity and differences in the chemical structure of these compounds may be reflected to the differences in biological actions between hypericin and Phx-1 or Phx-2.

Acknowledgments The present research was supported by funds from the Ito Foundation and from High-Tech Research Project for Private Universities: matching fund subsidy from the Ministry of Education, Culture, Sports, Science and Technology, Japan (2002—2006).

REFERENCES

1) Schaffer H. J., Beauchamp L., de Miranda P., Elion G. B., Bauer D. J., Collins P., *Nature* (London), **272**, 583—585 (1978).
2) Schmidtke M., Schnittler U., Jahn B., Dahse H., Stelzner A., *J. Virol. Methods*, **95**, 133—143 (2001).
3) Tomoda A., Yamaguchi J., Kojima H., Amemiya H., Yoneyama Y., *FEBS Lett.*, **196**, 44—48 (1986).
4) Tomoda A., Hamashima H., Arisawa M., Kikuchi T., Tezuka Y., Koshimura S., *Biochim. Biophys. Acta*, **1117**, 306—314 (1992).
5) Tomoda A., Arisawa M., Koshimura S., *J. Biochem.* (Tokyo), **110**, 1004—1007 (1991).
6) Mori H., Honda K., Ishida R., Nohira T., Tomoda A., *Anti-Cancer Drugs*, **11**, 653—657 (2000).
7) Koshibu-Koizumi J., Akazawa M., Iwamoto T., Takasaki M., Mizuno F., Kobayashi R., Abe A., Tomoda A., Hamatake M., Ishida R., *J. Cancer Res. Clin. Oncol.* **128**, 363—368 (2002).
8) Akazawa M., Koshibu-Koizumi J., Iwamoto T., Takasaki M., Nakamura M., Tomoda A., *Tohoku J. Exp. Med.*, **196**, 185—192 (2002).
9) Gao S., Takano T., Sada K., He J., Noda C., Hori-Tamura N., Tomoda A., Yamamura H., *Br. J. Pharmacol.*, **137**, 749—755 (2002).
10) Enoki E., Sada K., Qu X., Kyo S., Shahjahan Miah S. M., Hatani T., Tomoda A., Yamamura H., *J. Pharm. Sci.*, **94**, 329—333 (2004).
11) Iwata A., Yamaguchi A., Sato K., Izumi R., Tomoda A., *Tohoku J. Exp. Med.*, **200**, 161—165 (2003).
12) Kawamura H., Fujita T., Imada T., *Nippon Juigaku Zasshi*, **50**, 803—808 (1988).
13) Johnson K. L., Sarnow S. P., *J. Virol.*, **65**, 4341—4349 (1991).
14) Satoh K., Iwata A., Murata M., Hikata M., Hayakawa T., Yamaguchi T., *J. Virol. Methods*, **114**, 111—119 (2003).
15) Tang J., Colacino J. M., Larsen S. H., Spitzer W., *Antiviral Res.*, **13**, 313—326 (1990).
16) Huang H. C., Chu S. H., Chao P. D. L., *Eur. J. Pharmacol.*, **198**, 211—213 (1991).

[The 2nd Annual Meeting of JHUPO]

Two-dimensional electrophoretic analysis of disease-associated proteins in human cerebrospinal fluid from patients with rheumatoid arthritis

Yukio Yamamoto[1], Yoshiko Akita[1], Shigeyuki Tai[2], Susumu Fukasaku[3], Teruhide Yamaguchi[4], Tadashi Oshizawa[4], Kazuko Yamaoka[1], Mariko Shimamura[1] and Tadahiko Hazato[1]

SUMMARY

Comparing protein expression in the cerebrospinal fluid (CSF) of rheumatoid arthritis (RA) patients with that of controls, makes possible the uncovering of proteins that affect disease progression and regulate responsiveness to drugs. Two-dimensional gel electrophoresis (2-DE) and silver staining were used for identifying disease-associated CSF proteins in RA patients. First, to enhance the detection of CSF proteins and to improve the separation of their isoforms by 2-DE, CSF samples were pre-treated with an albumin and IgG removal kit, then by acetone precipitation. The 2-DE analysis revealed more than 1600 spots by the removal of albumin and immunoglobulin from CSF. The expression of the protein spots was not greatly changed in either group, but some notable changes in protein spots were observed in two RA samples. In particular, the expression of an approximately 50 kD protein increased markedly, whereas that of two sequential protein spots of 10–15 kD and with neutral pI decreased in the RA samples. These preliminary results suggest that the proteomic method is conducive to clarifying the mechanism of RA crises, and that some of the expression-changed proteins may be new candidates for disease-associated proteins of RA.

Key words: rheumatoid arthritis, cerebrospinal fluid, two-dimensional gel electrophoresis proteomics.

INTRODUCTION

Proteomics is a powerful tool in the search for potential proteins that function as biomarkers of various diseases. Identification of disease-associated proteins which are induced to change their expression compared with controls of particular diseases, and clarification of pathogenesis by two-dimensional gel electrophoresis(2-DE) and mass spectrometry have been reported[1–5]. Rheumatoid arthritis (RA) is a disease characterized by chronic polyarticular synovial inflammation and progressive destruction of cartilage and bone. A number of proteolytic enzymes (matrix metalloproteinases (MMP), cathepsins and peptidases) that degrade cartilage proteoglycans and collagen have demonstrated elevated levels in such tissues[6, 7]. Furthermore, interleukin-1β (IL-1β), tumor necrosis factor-α (TNF-α), various cytokines and inhibitors of enzymes also play significant roles in the pathogenesis of RA[8, 9]. These proteins, intricately associated with the knee and joint sites, turn malignant, leading to chronic inflammation and finally to the destruction of joints. Effective treatment is provided by several kinds of medication such as nonsteroidal anti-inflammatory drugs

[1] Tokyo Metropolitan Institute of Medical Science, Honkomagome 3-18-22, Bunkyo-ku, Tokyo 113-8613, Japan.
[2] Tokyo Metropolitan Bokutoh Hospital, Koutoubashi 4-23-15, Sumida-ku, Tokyo 130-8515, Japan.
[3] School of Medicine, Juntendo University, Hongo 2-1-1, Bunkyo-ku, Tokyo 113-8421, Japan.
[4] National Institute of Health Science, Kamiyoga 1-18-1, Setagaya,-ku, Tokyo 158-8501, Japan.
Corresponding address: Yukio Yamamoto, Ph.D., Department of Medical Biology, The Tokyo Metropolitan Institute of Medical Science, Honkomagome 3-18-22, Bunkyo-ku, Tokyo 113-8613, Japan.
Abbreviations: RA, rheumatoid arthritis; CSF, cerebrospinal fluid; 2-DE, two-dimensional gel electrophoresis.
JHUPO: Japan Human Proteome Organization
(Received July 2, 2004, Accepted january 13, 2005, Published March 15, 2005)

(NSAID), anti-rheumatoid drugs (DMARD) and biological reagents (anti-TNF receptor and IL-1 antagonist)[10-12]. Despite active treatment, however, numerous patients do not recover and continue to experience pain, sustain bone destruction and reach a chronic state.

Pain in RA, considered chronic and nociceptive, is stimulated in various nociceptors at peripheral sites (knee and joints), is a signal transduced through the spinal cord to the cerebrum and is conscious. A neuropeptide called spinorphin (LVVYPWT), an endogenous peptide derived from bovine spinal cord, which plays a role in anti-inflammatory and anti-nociceptive activity has been characterized[13, 14]. Furthermore to clarify the roles of spinorphin in inflammation and pain control, we focused on the changes in the activities of spinorphin and its metabolic enzymes in cerebrospinal fluids (CSF) of RA patients with chronic pain and inflammatory states. It is considered that changes in the protein composition of CSF may be reflected in alterations of the expressional pattern which is caused by the deterioration of disease in the central nervous system. The final goal of our study is to identify disease-associated proteins in the CSF of RA patients. In this study, the protein compositions in the CSFs from RA patients were analyzed by 2-dimensional gel electrophoresis (2-DE) and compared with those of controls.

MATERIALS AND METHODS

Materials

Tris(hydroxymethyl)aminomethane, tricine, iodoacetamide, thiourea, CHAPS and glycerol were purchased from Sigma-Aldrich Co. St Louise, MO, USA. Urea, 2-mercaptoethanol, dithiothreitol, methylenebisacrylamide and ampholine (pH 3.5–9.5) were purchased from Amersham Biosciences, Uppsala, Sweden. Sodium dodecyl sulfate (SDS), N,N,N',N'-tetramethylethylenediamine, glycerin, methanol and acetic acid were from Wako Chemical Ind., Ltd., Osaka, Japan. Silicone oil was from Shin-Etsu Silicone Chemical Co. Ltd., Tokyo, Japan. All other reagents were of electrophoresis grade.

Human cerebrospinal fluid

Cerebrospinal fluid (CSF) obtained from candidates for surgery under spinal anesthesia was studied. The diagnosis of RA was based on clinical criteria described in International Diagnostic Criteria[15]. The patients with RA (one man and one woman, 71 and 84 years old; mean, 77.5 years) had been treated with medication including anti-inflammatory drugs, gold, methotrexate, sulfasalazine, corticosteroids, bucillamine and D-penicillamine. Patients scheduled to undergo herniorrhaphy, ovariectomy or transurethral resection were designated as the control group (two women and three men; 37–87 years old; mean 59.8± 19.9 years); none of them had been treated with high doses of corticosteroids or intraarticular steroids. The study was approved by the Human Studies Committee, and informed consent was obtained from each patient.

Pre-treatment

Human CSF was pre-treated with an Albumin and IgG Removal kit (Amersham Biosciences UK Ltd., Little Chalfont, Buckinghamshire, UK) and with acetone precipitation according to the manufacturer's procedure. Briefly, 0.75 ml of the slurry included in the resin coated with specific antibodies was added to a tube containing 1 ml CSF and mixed. The mixture was rotated on a rotatory shaker for 60 min at room temperature, then centrifuged for 5 min at 6,500×g. The filtrate was collected and mixed with 4 volumes of ice-cold acetone. The proteins in the solution were allowed to precipitate at –20°C for at least 2 hrs. The solution was centrifuged at 13,000×g for 10 min; the protein pellets were then harvested, air-dried (typically 5–10 min at room temperature) and dissolved in lysis buffer (8 *M* urea, 2% ampholine (pH 3.5–9.5), 3% CHAPS, 4% glycerol and 4.5% 2-mercaptoethnol) for isoelectric focusing. Protein content was measured according to Bradford's method[16].

Isoelectric focusing (IEF)

IEF in the first dimension to separate the proteins according to their charge and strips (13 cm long; 3–10 pH non-linear range) were used. First-dimensional electrophoresis was conducted on a Multiphore II (Amersham Biosciences, Sweden) IEF system. Briefly, the lysis buffer was added to 50 μg pretreated CSF protein to a total volume of up to 250 μl. After direct rehydration of the IPG dry strip with the mixture, IEF was carried out on a stepwise program: 300 V for 6 h, 500 V for 1 h, 1000 V for 1 h, 1500 V for 1 h, 2000 V for 1 h, 2500 V for 1 h, 3000 V for 1 h, 3500 V for 36 h. After 1-D electrophoresis, the strips were stored at –80°C until 2-DE.

SDS-PAGE

The strip was first equilibrated twice for 15 min in a reducing equilibration buffer (6 *M* urea, 0.5 *M* Tris/HCl, pH 6.8, 25% glycerol, 2% SDS, a trace of bromophenol blue) containing 65 m*M* dithiothreitol and equilibrated again for 15 min with the equilibration buffer containing 135 m*M* iodoacetamide. SDS-polyacrylamide gel electrophoresis (SDS-PAGE) was then used in the second-dimensional electrophoresis at 20 mA for about 4–5 h, as described[17].

Silver staining

Because of its high sensitivity, silver staining was carried out for the detection of proteins with 2D-silver stain II-Daiichi (Daiichi Pure Chemicals Co. Ltd, Tokyo) according to the manufacturer's procedure.

RESULTS AND DISCUSSION

Effect of pretreatment

To analyze proteins associated with rheumatoid arthritis (RA), a disease characterized by chronic pain and immunological disorders, 2-DE was conducted on CSF samples. First, to obtain a high quality 2D pattern and reproducibility, CSF samples were pre-treated under several procedures. Albumins (constituting >50% of total protein content) and immunoglobulins (constituting >15% of total protein content)[18] were removed from CSF with an Albumin and IgG Removal kit, because the amounts of both major proteins varied among the samples and therefore the detection of minor components was difficult. The 2D profiles of the treated samples were then compared with those of the non-treated samples. Additional spots in 2-DE were visualized by this procedure (Fig. 1), although some spots which might be associated with albumin, were excluded. In particular, minor spots of 60–100 kD at neutral pI which were covered with albumin became clear and visible. Heavy and light chains of the IgG were also removed. The effect of another albumin removal kit (Montage Albumin Deplete kit, Millipore) for generating 2-D profiles was not as efficient as that of the above kit (the former removed only 50–60% of the albumin). We also examined the depletion of salts by acetone precipitation, TCA/acetone precipitation and a Clean-up kit (Amersham Bioscience (SF) Corp., CA, USA). The recovery of protein content was greater (about 1.5–2 fold) by acetone precipitation and the Clean-up kit than by the TCA/acetone precipitation. Effective procedures for removing salts are essential because the protein content in CSF is less than that in serum. We selected the acetone precipitation method for its higher yield and simpler application.

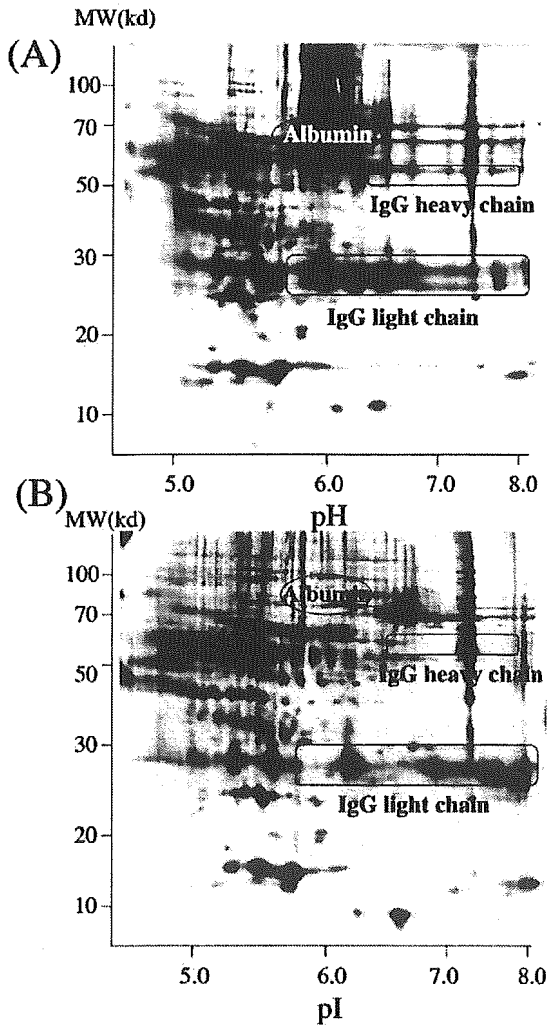

Fig. 1. Effect of pretreatment for albumin and IgG removal from cerebrospinal fluids.

2-DE profiles of (A) non-treated sample and (B) removal-kit-treated sample.

2-DE profile of CSF samples from patients with RA

To uncover disease-associated proteins in RA samples, 2D-profiles in the two RA and five controls were analyzed and compared. Serotransferrin (STF), prostaglandin-D synthase (PDS) and Transthyretin (TTR), which have specific expression in CSF and are used as reference markers[19] of CSF, were consistently detectable in both groups (Fig. 2 and Table 1). Macroscopic comparison of the 2D-profiles revealed several expression-changed proteins in the RA samples. Significantly, the expression of spots A and B decreased, whereas that of spot C increased in the RA samples compared with those in controls, except in one of five cases. The result was similar in both RA samples. Spots A and B consisted of several sequential components, which might be isoforms with several different charges modified by post-translational changes.

Table 1. Summary of characteristic proteins in CSF of patients with rheumatoid arthritis

	CSF Marker			A	B	C
	STF	TTY	PDS			
Con 1	+++	+++	+++	+	±	–
Con 2	+++	+++	+++	+++	–	–
Con 3	+++	+++	+++	++	±	++
Con 4	+++	+++	+++	+	±	–
Con 5	+++	+++	+++	+++	+++	–
RA 1	+++	+++	+++	–	–	++
RA 2	+++	+++	+++	–	–	++

The intensity of each spot was estimated by Phoretix 2D Advanced software and was classified to five-grade system as described below; – negative, ± faint, + weak, ++ moderate and +++ strong. STF is Serotransferrn, TTY is Transthyretin and PDS is Prostagrandin-D synthase.

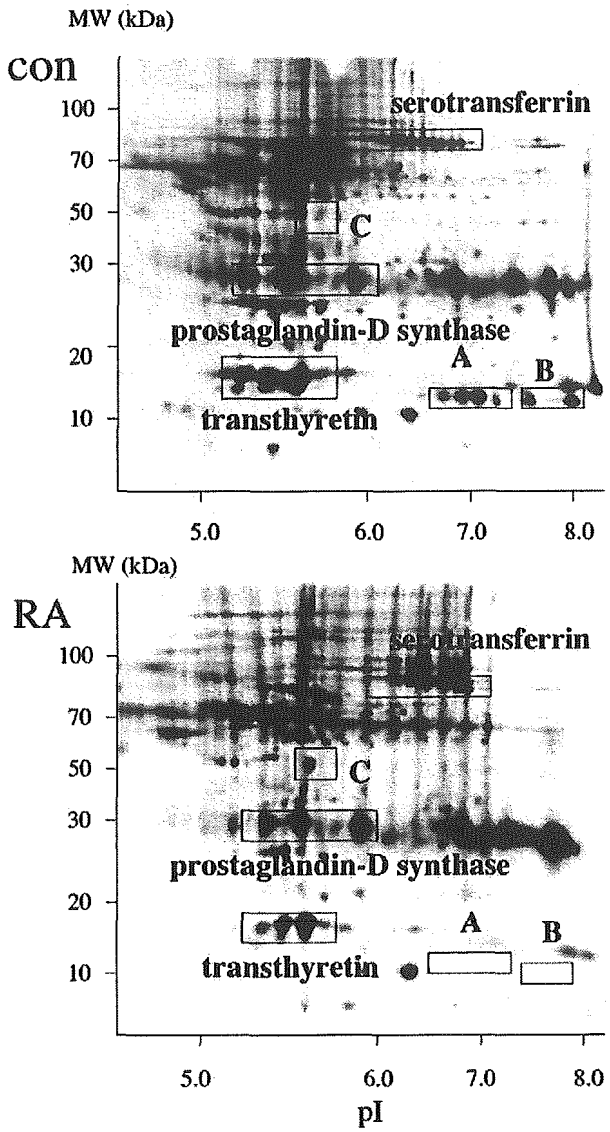

Fig. 2. 2-DE profile of proteins in cerebrospinal fluid (CSF) of patients with rheumatoid arthritis.

Serotransferrin, prostaglandin-D synthase and transthyretin are reference markers of human CSF. Rectangles represent spots of markedly expression-changed proteins. Con: CSF from control; RA: CSF from patients with RA.

It is reported that in the process of pathological and inflammatory states of RA, the levels of enzymatic activity of various proteinases and cytokine expression increase in the synovial fluid[6-9]. In this study, we have shown the changes in the several proteins in CSF of RA patients. Our results suggested that in the CSF besides in the synovial fluid, changes in the protein components which control pathophysiological change in the process of disease-deterioration. These proteins (spots A, B and C) have not been identified to date,but it would be interesting to clarify their relation to the pathology of disease. Spinorphin plays a role in the control of pain and inflammation in the body and changes have been observed in spinorphin levels and in the enzymatic activity of a spinorphin-processing enzyme, dipeptidyl peptidase III (DPPIII), in human cerebrospinal fluids[20]. When future studies clarify the relation between the pain-controlling system and the expression-changed proteins, the role of spinorphin as a new inhibitor in RA crises may be within reach.

In conclusion, our results suggest that this proteomic study is conducive to uncovering disease-associated proteins and to clarifying the mechanism of RA crises, and that the expression-changed proteins described in this study, may be new candidates in disease-associated proteins of RA. For more specific diagnostic and prognostic markers than those presently in use, additional data by comparisons between diseases and controls would be valuable.

ACKNOWLEDGEMENT

This work was supported in part by a Grant-in-Aid from the Ministry of Education, Science and Culture of Japan.

REFERENCES

1) Zheng PP, Luider TM, Pieters R, Avezaat CJ, van den Bent MJ, Sillevis Smitt PA, Kros JM. Identification of tumor-related proteins by proteomic analysis of cerebrospinal fluid from patients with primary brain tumors. J Neuropathol Exp Neurol 2003;62:855–862.
2) Davidsson P, Sjogren M, Andreasen N, Lindbjer M, Nilsson CL, Westman-Brinkmalm A, Blennow K. Studies of the pathophysiological mechanisms in frontotemporal dementia by proteome analysis of CSF proteins. Brain Res Mol Brain Res 2002;109:128–133.
3) Guillaume E, Zimmermann C, Burkhard PR, Hochstrasser DF, Sanchez JC. A potential cerebrospinal fluid and plasmatic marker for the diagnosis of Creutzfeldt-Jakob disease. Proteomics 2003;3:1495–1499.
4) Rohiff C. Proteomics in molecular medicine: Applications in central nervous systems disorders. Electrophoresis 2000;21:1227–1234.
5) Carrette O, Demalte I, Scherl A, Yalkinoglu O, Corthals G, Burkhard P, Hochstrasser DF, Sanchez JC. A panel of cerebrospinal fluid potential biomakers for the diagnosis of Alzheimer's disease. Proteomics 2003;3:1486–1494.
6) Landewe R, Geusens P, Boers M, van der Heijde D, Lems W, te Koppele J, van der Linden S, Garnero P. Markers for type II collagen breakdown predict the effect of disease-modifying treatment on long-term radiographic progression in patients with rheumatoid arthritis. Arthritis Rheum 2004;50:1390–1399.
7) Tchetverikov I, Lard LR, DeGroot J, Verzijl N, TeKoppele JM, Breedveld FC, Huizinga TW, Hanemaaijer R. Matrix metalloproteinases-3, -8, -9 as markers of disease activity and joint damage progression in early rheumatoid arthritis. Ann Rheum Dis 2003;62:1094–1099.
8) Cross A, Edwards SW, Bucknall RC, Moots RJ. Secretion of oncostatin M by neutrophils in rheumatoid arthritis. Arthritis Rheum 2004;50:1430–1436.
9) Raap T, Justen H-P, Miller LE, Cutoro M, Scholmerich J, Straub RH. Neurotransmitter modulation of interleukin 6

(IL-6) and IL-8 (IL-8) secretion of synovial fibroblasts in patients with rheumatoid arthritis compared to osteoarthritiss. J Rhumatol 2000;27:2558–2565.
10) Klimiuk PA, Sierakowski S, Domyslawska I, Chwiecko J. Effect of repeated infliximab therapy on serum matrix metalloproteinases and tissue inhibitors of metalloproteinases in patients with rheumatoid arthritis. J Rheumatol 2004;31:238–242.
11) Dougados M, Emery P, Lemmel EM, de la Serna R, Zerbini CA, Brin S, van Riel P. Efficacy and safety of leflunomide and predisposing factors for treatment response in patients with active rheumatoid arthritis: RELIEF 6-month data. J Rheumatol 2003;30:2572–2579.
12) De A, Blotta HM, Mamoni RL, Louzada P, Bertolo MB, Foss NT, Moreira AC, Castro M. Effects of dexamethasone on lymphocyte proliferation and cytokine production in rheumatoid arthritis. J Rheumatol 2002;29:46–51.
13) Yamamoto Y, Kanazawa T, Shimamura M, Ueki M, Hazato T. Inhibitory action of spinorphin, an endogenous regulator of enkephalin degrading enzymes, on carrageenan-induced polymorphonuclear neutrophil accumulation in mouse air-pouches. Life Sciences 1998;62:1767–1773.
14) Yamamoto Y, Ono H, Ueda H, Shimamura M, Nishimura K, Hazato T. Spinorphin as an endogenous inhibitor of enkephalin-degrading enzymes: Roles in Pain and Inflammation. Current Protein and Peptide Science 2002;3:587–599.
15) Arnett FC, Edworthy SM, Bloch DA. The American Rheumatism Association 1987 received criteria for the classificqation of rheumatoid arthritis. Arthritis Rheum 1988;31:315–324.
16) Bradford MM. A rapid and sensitive method for the quantitation of microgram quantities of protein utilizing the principle of protein-dye binding. Anal Biochem 1976;72: 248–254.
17) Toda T. Standardization of protocol for Immobiline 2-D PAGE and construction of 2-D PAGE protein database on World Wide Web home page. Jpn J Electrophoresis 1997; 41:13–20.
18) Yuan X, Russel T, Wood G, Desiderio DM. Analysis of the human lumbar cerebrospinal fluid proteome. Electrophoresis 2002;23:1185–1196.
19) Burkhard PR, Rodrigo N, May D, Sztajzel R, Sanchez J-C, Hochstrasser DF, Schiffer E, Reverdin A, Lacroix JS. Assessing cerebrospinal fluid rhinorrhea: A two-dimensional electrophoresis approach. Electrophoresis 2001;22: 1826–1833.
20) Yamamoto Y, Sato H, Fukasaku S, Hiramatsu K, Tai S, Shimamura M, Hazato T. Levels of spinorphin in cerebrospinal fluid derived from patients with pain increase with decreasing dipeptidyl peptidase III. Pain Research in press.

NOTE *Clinical Pathology*

Polymorphisms of Caprine PrP Gene Detected in Japan

Yasuhisa KUROSAKI[1], Naotaka ISHIGURO[2]*, Motohiro HORIUCHI[3] and Morikazu SHINAGAWA[4]

[1]*Laboratory of Veterinary Public Health, Obihiro University of Agriculture and Veterinary Medicine, Obihiro, Hokkaido 080–8555,* [2]*Laboratory of Food and Environmental Hygiene, Faculty of Applied Biological Sciences, Gifu University, 1–1 Yanagido, Gifu 501–1193,* [3]*Laboratory of Prion Diseases, Graduate School of Veterinary Medicine, Hokkaido University, Sapporo 060–0818 and* [4]*Prion Disease Research Center, National Institute of Animal Health, 3–1–5 Kannondai, Tsukuba, Ibaragi 305–0856, Japan*

(Received 18 August 2004/Accepted 5 November 2004)

ABSTRACT. Polymorphism of the PrP gene is a primary factor influencing susceptibility and incubation period in natural and experimental scrapie in sheep and goats. Polymorphisms of the caprine PrP gene in Japan were examined in 118 goats. Eight allelic variants and 19 genotypes were obtained. Amino acid polymorphisms were observed at 7 codons: 102, 142, 143, 240, 127, 146 and 211 (the latter 3 are novel polymorphisms). The polymorphisms at codons 142M and 143R, which are associated with the resistance to scrapie, were relatively rare in the present study. Thus, the present results provide information about the caprine PrP gene that may be useful for assessing the risk of goat scrapie.

KEY WORDS: goat, polymorphism, PrP.

J. Vet. Med. Sci. 67(3): 321–323, 2005

Scrapie is a fatal and infectious neurodegenerative disease that occurs in sheep and goats. Like bovine spongiform encephalopathy (BSE) in cattle and Creutzfeld-Jakob disease (CJD) in humans, scrapie is a transmissible spongiform encephalopathy (TSE). TSEs are characterized by accumulation of an abnormal isoform (PrP^{Sc}) of a normal cellular prion protein (PrP^{C}) in the central nervous system [12].

Among animals with natural or experimental scrapie, there is considerable variation in susceptibility and incubation period, even when the animals are exposed to the same infectious agent simultaneously [1, 4, 9]. Studies have shown that interaction between the scrapie strain and the PrP genotype in the affected animals plays a primary role in differences in infectivity [4, 8]. Polymorphisms of the open reading frame (ORF) of the cellular PrP gene significantly influence the incidence of natural scrapie [1, 9]. Amino acid polymorphisms of the sheep PrP gene have been observed at the following codons: 112 (M→T), 136 (A→V), 137 (M→T), 138 (S→N), 141 (L→F), 151 (R→C), 154 (R→H), 171 (Q→H or Q→R), 176 (K→N), and 211 (R→Q). The amino acid polymorphism at codon 171 is strongly associated with incubation period in many breeds of sheep [1, 4, 7, 9, 10, 14].

Goats as well as sheep are natural hosts for scrapie. The clinical signs of affected goats are slightly different from those of sheep, but the observed variation of incubation period is similar to that described for sheep [11, 14]. Studies have shown amino acid polymorphisms of the caprine PrP gene at the following codons: 21 (V→A), 23 (L→P), 49 (G→S), 102 (W→G), 142 (I→M), 143 (H→R), 154 (R→H), 168 (P→Q), 220 (Q→H) and 240 (S→P) [2, 3, 5, 6, 11].

In Japan, caprine scrapie has not yet been observed, although occurrence of sheep scrapie in Japan has been reported [10, 13]. In the present study, we investigated polymorphisms of the PrP gene in goats raised in Japan, to obtain genetic information for use in assessing the risk of the occurrence of scrapie in goats.

A total of 118 samples (48 tonsillar samples and 70 blood samples) were collected from healthy goats in Japan (Table 1). The 48 tonsillar samples were collected from Honshu Island, the Hachijo Islands and Hokkaido Island for TSE surveillance. The 70 blood samples were collected from goats in the Hachijo Islands (32 samples) and Okinawa Island (38 samples). Most of the goats from which samples were obtained were of the Saanen breed or related breeds.

DNA extraction from the 48 tonsillar samples and 70 blood samples was performed using the DNeasy Tissue Kit and QIAamp DNA Blood Mini Kit (QIAGEN Science, MD), respectively.

For polymerase chain reaction (PCR) and sequencing of the caprine PrP gene, the sheep primer sets SPrP-1/SP-4 and SP-1/SPrP 2 were used to amplify the upstream region (approximately 430 bp) and downstream region (approximately 370 bp) of the PrP gene, respectively [7]. The over-

Table 1. Sampling sites and caprine PrP allele variations

Sampling Sites	Number of goats	PrP allelic variants (%)
Hokkaido Island	1	1(50), 8(50)
Honshu Island	6[a)]	1(42), 2(25), 6(8), 8(25)
Hachijyo Island	73	1(44), 2(38), 5(2), 6(1), 8(15)
Okinawa Island	38	1(34), 2(33), 3(3), 4(1), 5(11), 6(8), 7(5), 8(5)

a)Aomori prefecture (3 samples), Miyagi prefecture (1 sample), Hiroshima prefecture (1 sample) and Tokyo (1 sample).

* CORRESPONDENCE TO: Dr. ISHIGURO, N., Laboratory of Food and Environmental Hygiene, Faculty of Applied Biological Sciences, Gifu University, 1–1 Yanagido, Gifu 501–1193, Japan.

Table 2. Variations of caprine PrP gene

Allele	PrP codon[a]							Number
	102	127	142	143	146	211	240	goats
1[b]	W	G	I	H	N	R	S	99
2	–	–	–	–	–	–	P	82
3	G	–	–	–	–	–	–	2
4	–	S	–	–	–	–	P	1
5	–	–	M	–	–	–	P	11
6	–	–	–	R	–	–	P	7
7	–	–	–	–	S	–	P	4
8	–	–	–	–	–	Q	–	30
Total								236
Genotype								
1/1	WW	GG	II	HH	NN	RR	SS	22
1/2	WW	GG	II	HH	NN	RR	SP	31
2/2	WW	GG	II	HH	NN	RR	PP	17
1/3	WG	GG	II	HH	NN	RR	SS	1
2/3	WG	GG	II	HH	NN	RR	SP	1
2/4	WW	GS	II	HH	NN	RR	PP	1
1/5	WW	GG	IM	HH	NN	RR	SP	4
5/8	WW	GG	IM	HH	NN	RQ	SP	1
2/5	WW	GG	IM	HH	NN	RR	PP	3
5/5	WW	GG	MM	HH	NN	RR	PP	1
5/6	WW	GG	IM	HR	NN	RR	PP	1
1/6	WW	GG	II	HR	NN	RR	SP	5
1/2	WW	GG	II	HR	NN	RR	PP	3
6/7	WW	GG	II	HR	NS	RR	PP	1
1/7	WW	GG	II	HH	NS	RR	SP	2
2/7	WW	GG	II	HH	NS	RR	PP	1
1/8	WW	GG	II	HH	NN	RQ	SS	9
2/8	WW	GG	II	HH	NN	RQ	SP	8
8/8	WW	GG	II	HH	NN	QQ	SS	6
Total								118

a) Amino acids are described as the single letter: W,tryptohan; G, glycine; S, serine; I, isoleucine; M, methionine; H, histidine; R, arginine; N, asparagine; Q, glutamine acid; P, proline.
b) Wild type of sheep.

lapping region of the 2 amplified fragments was approximately 40 bp. PCR amplification and DNA sequencing were performed as described previously [7]. To verify novel polymorphisms of the caprine PrP gene detected by direct sequencing, cloning of the caprine PrP gene to a vector plasmid was performed as described previously [7]. Five colonies possessing the recombinant plasmid were selected, and their plasmid DNAs were prepared using a Plasmid Mini Kit (QIAGEN Science) and sequenced as described previously [7].

Nine polymorphisms of the DNA sequence of the caprine PrP gene were detected (Table 2). Two of those polymorphisms (at codons 42 and 138) were silent mutations, and the remaining 7 polymorphisms (at codons 102, 127, 142, 143, 146, 211 and 240) caused amino acid changes. Three of the amino acid substitutions detected in the present study were novel polymorphisms: at codon 127, a g→a nucleotide substitution in the first codon position caused an amino acid change of G→S; at codon 146, an a→g nucleotide substitution in the second position caused an amino acid change of N→S; at codon 211, a g→a nucleotide substitution caused an amino acid change of R→Q. The remaining 4 amino acid polymorphisms detected in the present study have previously been described: codon 102, W→G; codon 142, I→M; codon 143, H→R; codon 240, S→P [2, 5, 6, 11].

The present distinctive amino acid polymorphisms at 7 codons comprised 8 allelic variations and 19 different genotypes (Table 2). Alleles 1 and 2 are the predominant alleles of the caprine PrP gene in Japan. Genotype 1/1 has been identified in wild-type sheep in Japan, and genotypes 1/2 and 2/2 are commonly observed in goats in Japan. These 3 genotype groups are distinguished by alteration of codon 240, and accounted for 59% of the 118 present samples.

To estimate the genetic background of goats from Okinawa, Hachijo, Honshu and Hokkaido Islands, allelic variants were classified along with the sampling sites (Table 1). All allelic variations detected in the present study occurred in goats from Okinawa Island. Goats from Honshu and the Hachijo Islands possessed 2 major alleles (1 and 2) and the minor alleles 5, 6 and 8. Goats in Okinawa Island have been frequently introduced from several prefectures in Honshu Island, so that allelic variants were obviously detected.